of scales resolved by modern cloud models, space-based remote sensing is an ever more necessary part of model validation.

Finally, a new approach is to use cloud-resolving models in place of traditional cumulus parameterizations in large-scale models. This explicit approach, called cloud-resolving convection parameterization or super-parameterization, alleviates several uncertainties associated with parameterization. Experimental at present, it has the potential to be viable in operational prediction models as advances continue to be made in computer technology and processing speed.

See also

Air–Sea Interaction: Momentum, Heat and Vapor Fluxes. **Boundary Layers:** Modeling and Parameterization. **Cloud Microphysics**. **Convection:** Convection in the Ocean. **Convective Storms:** Overview. **Density Currents**. **Diurnal Cycle**. **Mesoscale Meteorology:** Mesoscale Convective Systems; Models; Overview. **Numerical Models:** Methods. **Parameterization of Physical Processes:** Clouds. **Radiative Transfer:** Cloud-radiative Processes. **Satellite Remote Sensing:** Cloud Properties; Precipitation. **Thermodynamics:** Saturated Adiabatic Processes. **Tropical Meteorology:** Overview and Theory. **World Climate Research Program**.

Further Reading

Cotton WR and Anthes RA (1989) *Storm and Cloud Dynamics*. International Geophysics Series, Vol. 44. San diego: Academic Press.

Grabowski WW and Moncrieff MW (2001) Large-scale organization of tropical convection in two-dimensional explicit numerical simulations. *Quarterly Journal of the Royal Meteorological Society* 127: 445–468.

Houze RA Jr (1993) *Cloud Dynamics*. International Geophysics Series, Vol. 53. San Diego: Academic Press.

Ludlam FH (1980) *Clouds and Storms: The Behavior and Effect of Water in the Atmosphere*. University Park: The Pennsylvania State University Press.

Moncrieff MW and Tao W-K (1999) Cloud-resolving models. In: Browning K and Gurney RJ (eds) *Global Water and Energy Cycles*, pp. 200–209. Cambridge: Cambridge University Press.

Smith RK (1997) *The Physics and Parameterization of Moist Atmospheric Convection*. NATO Advanced Study Institute Series C: Mathematical and Physical Sciences, vol. 505.

CONVECTIVE STORMS

Contents

Overview

M L Weisman, National Center for Atmospheric Research, Boulder, CO, USA

Introduction

Convective storms, also commonly referred to as thunderstorms, produce some of the fiercest weather on earth, including flooding rains (with rain rates up to several inches or 100 mm h^{-1}), severe surface winds (sometimes reaching magnitudes greater than 100 kn), hail (reaching the size of grapefruit), frequent lightning, and tornadoes. Individual convective cells are generally observed on scales of 5–30 km, and can have lifetimes ranging from 30–40 min to greater than 6 h. Furthermore, groups of convective cells can become organized into larger mesoscale convective systems, such as squall lines, bow echoes, and mesoscale convective complexes, which can extend over hundreds of kilometers and, in some cases, can last for several days.

Convective storms exist under a wide variety of conditions and evolve in an equally wide variety of ways. Storm behavior is inherently dependent on the environment in which the storm grows, including thermodynamic stability, vertical wind profiles, and mesoscale forcing influences. In the following, we review the properties of the most basic storm types, including the ordinary cell, multicell, and supercell, and explain the fundamental physical processes that promote the various storm behaviors. Our knowledge of convective storms is based largely on extensive

of scales resolved by modern cloud models, space-based remote sensing is an ever more necessary part of model validation.

Finally, a new approach is to use cloud-resolving models in place of traditional cumulus parameterizations in large-scale models. This explicit approach, called cloud-resolving convection parameterization or super-parameterization, alleviates several uncertainties associated with parameterization. Experimental at present, it has the potential to be viable in operational prediction models as advances continue to be made in computer technology and processing speed.

See also

Air–Sea Interaction: Momentum, Heat and Vapor Fluxes. **Boundary Layers:** Modeling and Parameterization. **Cloud Microphysics**. **Convection:** Convection in the Ocean. **Convective Storms:** Overview. **Density Currents**. **Diurnal Cycle**. **Mesoscale Meteorology:** Mesoscale Convective Systems; Models; Overview. **Numerical Models:** Methods. **Parameterization of Physical Processes:** Clouds. **Radiative Transfer:** Cloud-radiative Processes. **Satellite Remote Sensing:** Cloud Properties; Precipitation. **Thermodynamics:** Saturated Adiabatic Processes. **Tropical Meteorology:** Overview and Theory. **World Climate Research Program**.

Further Reading

Cotton WR and Anthes RA (1989) *Storm and Cloud Dynamics*. International Geophysics Series, Vol. 44. San diego: Academic Press.

Grabowski WW and Moncrieff MW (2001) Large-scale organization of tropical convection in two-dimensional explicit numerical simulations. *Quarterly Journal of the Royal Meteorological Society* 127: 445–468.

Houze RA Jr (1993) *Cloud Dynamics*. International Geophysics Series, Vol. 53. San Diego: Academic Press.

Ludlam FH (1980) *Clouds and Storms: The Behavior and Effect of Water in the Atmosphere*. University Park: The Pennsylvania State University Press.

Moncrieff MW and Tao W-K (1999) Cloud-resolving models. In: Browning K and Gurney RJ (eds) *Global Water and Energy Cycles*, pp. 200–209. Cambridge: Cambridge University Press.

Smith RK (1997) *The Physics and Parameterization of Moist Atmospheric Convection*. NATO Advanced Study Institute Series C: Mathematical and Physical Sciences, vol. 505.

CONVECTIVE STORMS

Contents

Overview

M L Weisman, National Center for Atmospheric Research, Boulder, CO, USA

Introduction

Convective storms, also commonly referred to as thunderstorms, produce some of the fiercest weather on earth, including flooding rains (with rain rates up to several inches or 100 mm h^{-1}), severe surface winds (sometimes reaching magnitudes greater than 100 kn), hail (reaching the size of grapefruit), frequent lightning, and tornadoes. Individual convective cells are generally observed on scales of 5–30 km, and can have lifetimes ranging from 30–40 min to greater than 6 h. Furthermore, groups of convective cells can become organized into larger mesoscale convective systems, such as squall lines, bow echoes, and mesoscale convective complexes, which can extend over hundreds of kilometers and, in some cases, can last for several days.

Convective storms exist under a wide variety of conditions and evolve in an equally wide variety of ways. Storm behavior is inherently dependent on the environment in which the storm grows, including thermodynamic stability, vertical wind profiles, and mesoscale forcing influences. In the following, we review the properties of the most basic storm types, including the ordinary cell, multicell, and supercell, and explain the fundamental physical processes that promote the various storm behaviors. Our knowledge of convective storms is based largely on extensive

radar studies (using both conventional and Doppler radars) as well as numerical cloud modeling studies. More information on convective storms can also be obtained from related chapters on lightning, hail, tornadoes, mesoscale convective systems, bow echoes, convective storm modeling, and severe weather forecasting.

Observed Convective Storm Types

The concept of the convective cell is fundamental to a discussion of convective storms. The convective cell will be regarded as a region of strong updraft (greater than $5\,m\,s^{-1}$) and associated precipitating downdraft having a horizontal cross-section of 10–100 km^2, and extending in the vertical through most of the troposphere. Intense convective cells can have updrafts greater than $60\,m\,s^{-1}$, with downdrafts sometimes greater than $30\,m\,s^{-1}$. Research has shown that convective cells as observed on radar often evolve in identifiable, repeatable patterns. On the basis of these radar characteristics, conceptual models have been proposed for the most commonly observed storm types. These include the short-lived ordinary cell, multiple cell systems or 'multicell', and supercell.

Ordinary-Cell Storm

The ordinary cell represents the most basic convective storm type (**Figure 1**). It consists of a single updraft, which rises rapidly through the troposphere in a conditionally unstable atmosphere, producing large amounts of liquid water and ice. When the raindrops or ice particles become too heavy for the updraft to support, they begin to fall, creating a downdraft that quickly replaces the updraft. The downdraft is initially nearly saturated, but as it falls into the lower troposphere and mixes with drier air, strong evaporational cooling may occur. This cooling accelerates the downdraft (because of negative buoyancy), which spreads out horizontally as a cold pool (gust front) on reaching the surface. If the diverging outflow winds reach severe levels (greater than about 50 kn), the event is referred to as a downburst or microburst. This life cycle (**Figure 1**) usually takes 30–50 min to complete, and generally severe weather such as high winds or hail tends to be short-lived. Relatively weak, short-lived tornadoes do occasionally occur with ordinary cells, and are sometimes referred to as landspouts or non-supercell tornadoes.

Multicell Storm

The multicell storm can be thought of as a cluster of short-lived ordinary cells. The cold outflows from each cell, however, combine to form a large gust front, the convergence and lifting along its leading edge being generally strongest in the downshear direction relative to the low-level (0–3 km agl) vertical wind shear vector. In most cases, this also happens to be in the direction of storm motion. This convergence and lifting can trigger new updraft development along and

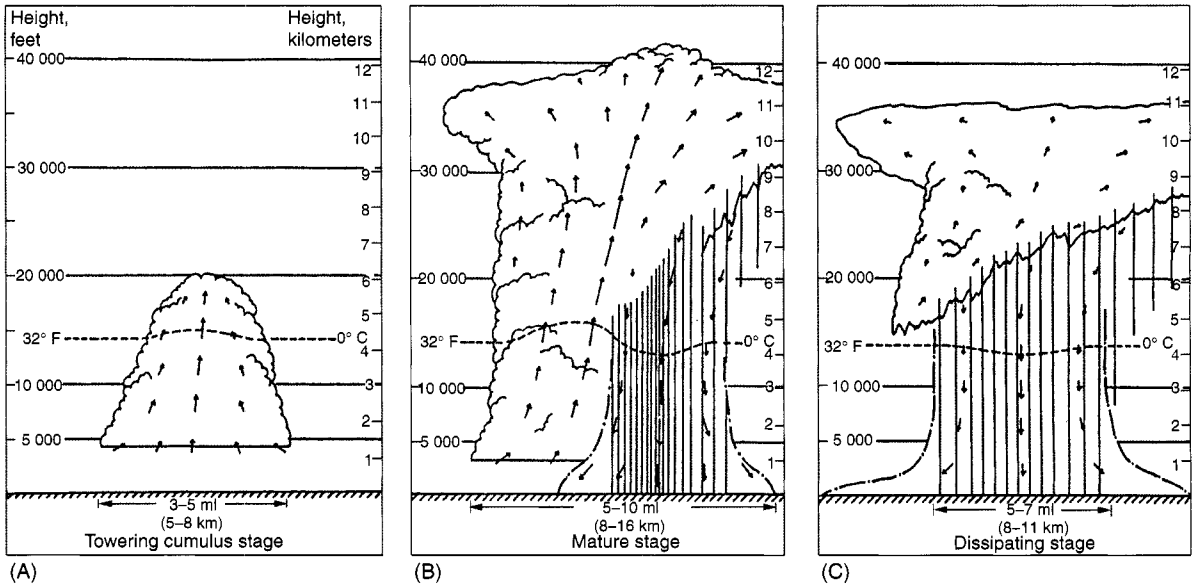

Figure 1 (A) Towering cumulus stage, (B) mature stage, and (C) dissipating stage of an 'ordinary' convective cell. (Courtesy of CA Doswell. Adapted with permission from Byers HR and Braham RR Jr (1949) *The Thunderstorm*. Supt of Documents. Washington DC: US Government Printing Office.

just behind the gust front, and new cells evolve as described in the previous subsection. **Figure 2** shows this process in a vertical cross-section through a multicellular hailstorm observed during the National Hail Research Experiment. The new cell growth often appears disorganized, but occasionally occurs on a preferred storm flank. Because of their ability to renew themselves constantly through new cell growth, multicell storms often last many hours, affecting areas thousands of square kilometers. If the storm motion is very slow, heavy local rainfall may occur, presenting the possibility of flooding. Severe surface winds in the form of downbursts or microbursts can occur with multicell storm systems, with hail and tornadoes also possible in the vicinity of strong updraft centers.

Supercell Storm

The supercell is potentially the most dangerous convective storm, often producing high winds, large hail, and long-lived tornadoes. In its purest form it consists of a single, quasi-steady, rotating updraft and associated downdraft, which may have a lifetime of several hours. It often evolves from multicell storm systems, and even during its quasi-steady phase may comprise several small-scale rain centers embedded within a larger encompassing cellular structure. However, the general structure and evolution of the supercell suggest that it is dynamically different from ordinary convection.

A schematic of a supercell is presented in **Figure 3**. Unlike ordinary cells or multicell systems, supercells are often characterized by a persistent separation between the primary updraft and downdraft currents. The updraft region is generally found on the upshear side of the cloud, and is characterized by a well-defined cloud base with rapidly growing cloud turrets above. This portion of the storm often exhibits pronounced cyclonic rotation. The downdraft region is found primarily downshear of the updraft region, appearing more diffuse due to the heavy precipitation. The anvil spreads predominantly downshear aloft, but in stronger storms also extends upshear somewhat as the divergence near the storm top is able to force itself upstream against the strong upper-level flow. Overshooting tops are quite common for the stronger storms. Many supercells also display a stair-step-shaped flanking line extending upshear from the storm's main updraft region. A persistent lowering of the cloud base, referred to as a wall cloud, is also often

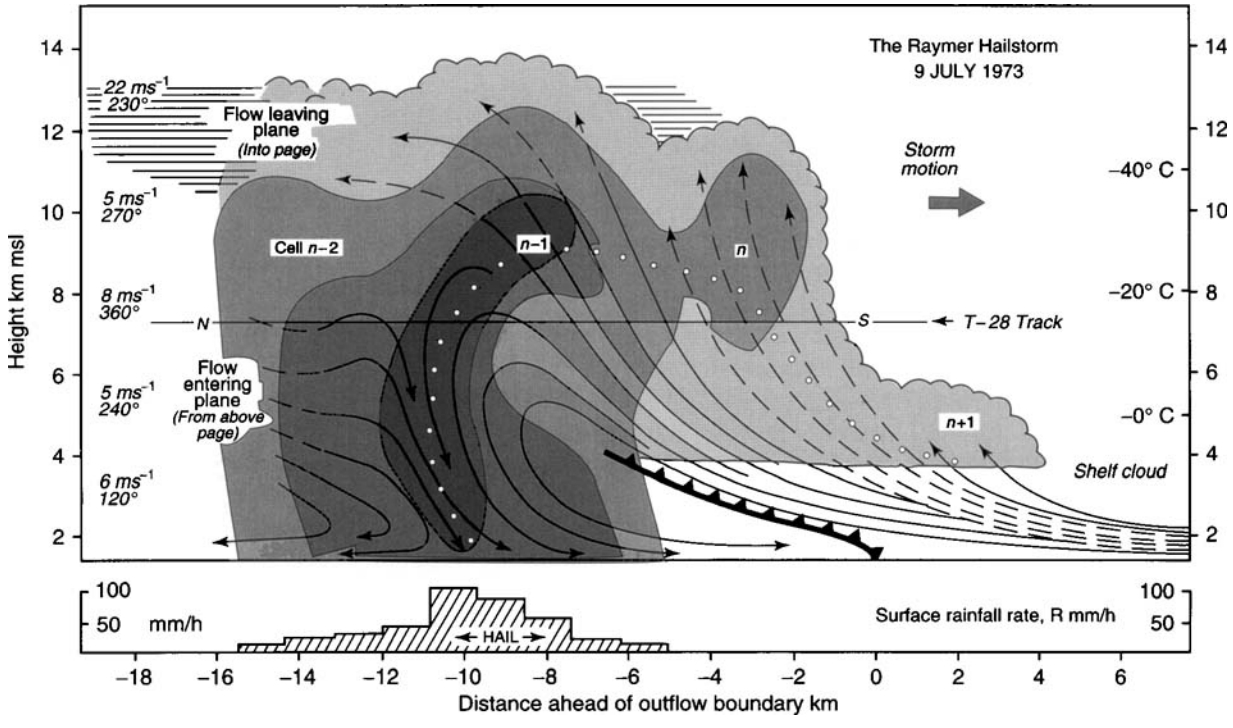

Figure 2 Vertical cross-section through a multicell hailstorm, along the storm's direction of travel through a series of evolving cells ($n-2$, $n-1$, n, $n+1$). The solid lines are streamlines of flow relative to the moving system; on the left their broken ends represent flow into and out of the plane, and on the right they represent flow remaining within a plane a few kilometers closer to the reader. Light shading represents the extent of the cloud, and the three darker shades represent radar reflectivities of 35, 45, and 50 dBZ. (Reproduced with permission from Browning KA, Fankhauser JC, Chalon J-P, *et al.* (1976) Structure of an evolving hailstorm. Part V: Synthesis and implications for hail growth and hail suppression. *Monthly Weather Reviews* 104: 603–610.)

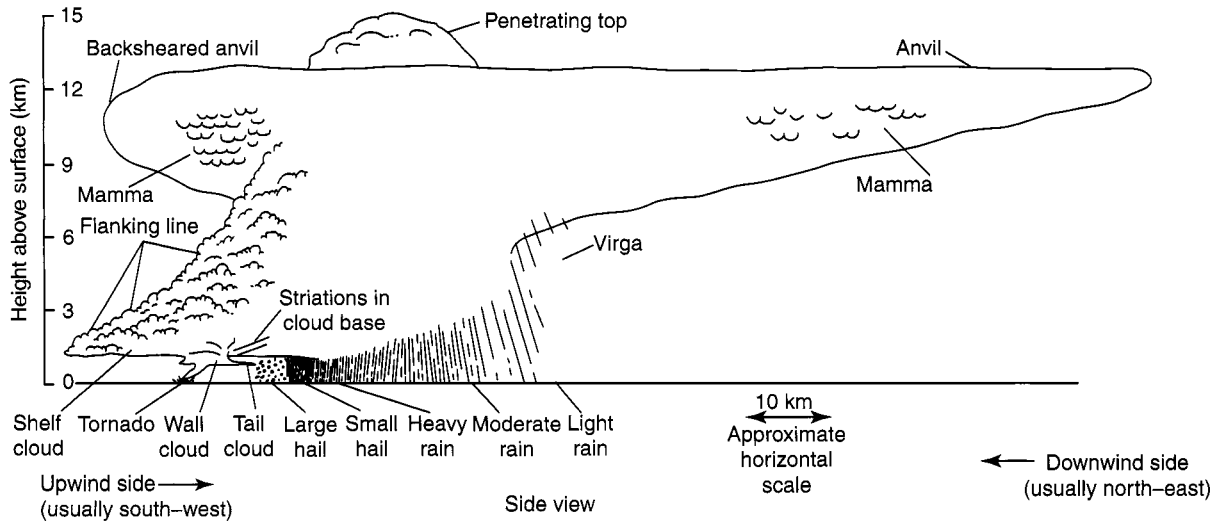

Figure 3 Schematic visual view of a mature supercell thunderstorm. (Reproduced with permission from Bluestein HB and Parks CR (1983) A synoptic and photographic climatology of low-precipitation severe thunderstorms in the southern plains. *Monthly Weather Reviews* 111: 2034–2046.)

observed beneath the main updraft region of the storm, and is often a precursor to the development of tornadoes.

The structure of a mature supercell as it might be observed on radar is depicted in **Figure 4**. The reflectivity field tends to be elongated in the direction of the mean vertical wind shear, with a hooklike appendage often appearing on the south-west flank of the storm. The midlevel reflectivity often overhangs the low-level echo, and often a bounded weak echo region (BWER) appears at middle levels above the edge of the low-level reflectivity gradient. A BWER usually indicates the presence of both strong updraft and strong rotation about a vertical axis in its vicinity.

Figure 5 presents the significant surface features commonly observed during a supercell's mature phase. The main updraft region is found straddling the hook or notch in the rain field, with two primary downdraft regions, referred to the forward flank downdraft and rear flank downdraft, located on the downshear and upshear sides of the updraft, respectively. A surface gust front separates the cool, rainy air from the warm ambient air, with the gust front often wrapped around the southern flank of the storm due to the circulation associated with a surface mesocyclone. This rear flank gust front can overtake the gust frontal boundary associated with the forward flank downdraft, creating an occlusion of these frontal features. A tornado, if present, often forms at the tip of this occlusion (on the edge of the hook echo) on the gradient between updraft and downdraft (but within the updraft).

A time series of radar reflectivity structure for a storm that occurred on 19 April 1972 near Norman, OK (**Figure 6**) portrays a commonly observed trait of supercell storms. About 1 h into the storm's lifetime, the rain center appears to split into two diverging echo masses: the more intense southern storm veers to the right and slows its motion, while the northern storm moves more quickly to the north-east. Such storm splitting is common in association with supercell storms. The right mover (right relative to the direction of the ambient shear vector) is associated with a cyclonically rotating updraft while the left mover is associated with an anticyclonically rotating updraft. Both right and left movers of a splitting storm are apt to produce severe weather such as hail and high winds, but tornadoes are rarely associated with left-moving storms.

Physical Mechanisms Controlling Convective Storm Growth and Evolution

Convective storm type and severity are strongly dependent on the environmental conditions in which the storm grows. Of particular importance is the thermodynamic instability (buoyancy) and vertical wind shear. Thermodynamic instability exerts a fundamental control on convective storm strength, as it controls the vertical acceleration of air parcels. Vertical wind shear, however, influences strongly the form that the convection might take, i.e., whether the convection evolves as short-lived ordinary cells,

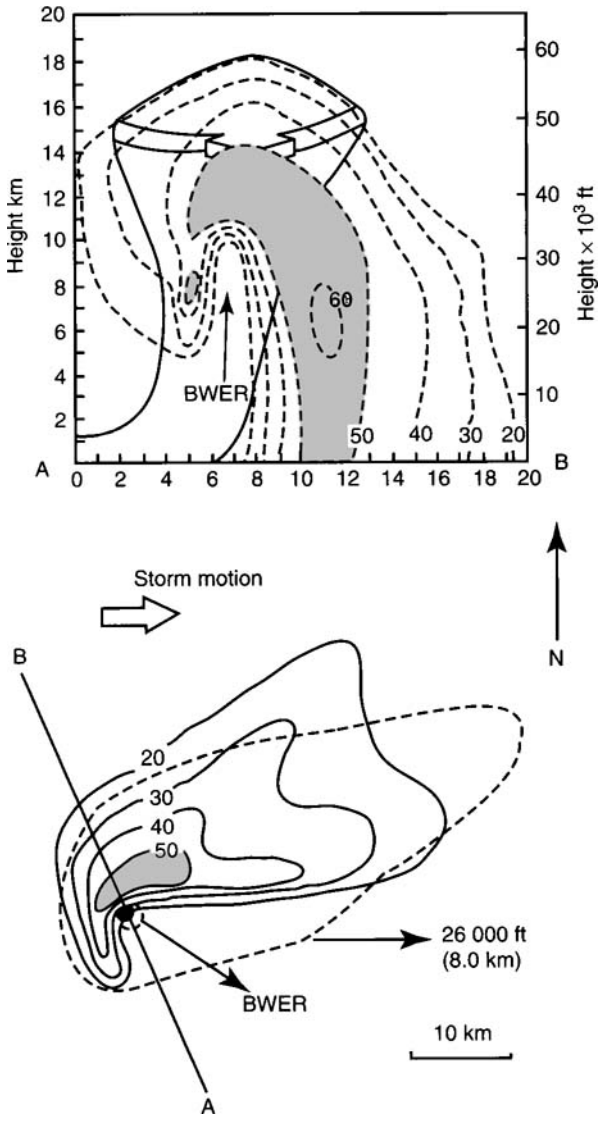

Figure 4 (Above) Vertical cross-section as might be observed on a radar scope during the mature phase of an intense supercell storm. Low-level inflow, updraft, and outflow aloft (solid lines) are superimposed on the radar reflectivity (dashed lines). (Below) Composite tilt sequence. Solid lines are the low-level reflectivity contours, dashed lines outline the echo greater than 20 dBZ derived from the middle-level elevation scan, and the black dot is the location of the maximum top from the high-level scan. (Adapted with permission from Lemon LR (1980) *Severe Thunderstorm Radar Identification Techniques and Warning Criteria*. NOAA Technical Memorandum, NWS NSSFC-3, Kansas City, MO (NTIS PB81-234809).

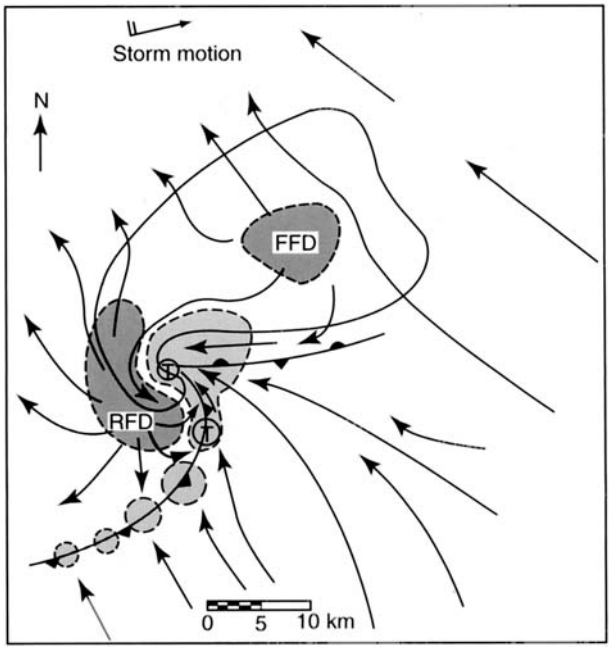

Figure 5 Schematic plan view of a tornadic supercell thunderstorm at the surface. The thick line encompasses radar echo. The thunderstorm wavelike 'gust front' structure is also depicted by use of a solid line and frontal symbols. Surface positions of the updraft are finely stippled; forward flank downdraft (FFD) and rear flank downdraft (RFD) are coarsely stippled; along with associated streamlines (relative to the storm). Likely tornado locations are shown by encircled T's. The major cyclonic tornado is most probable at the wave apex, while a minor cyclonic tornado may occur at the bulge in the cold front (southern T), which also marks the favored location for new mesocyclone. Anticyclonic tornadoes, if any, are found even farther south along the cold front. (Reproduced with permission from Davies-Jones RP (1985) *Tornado Dynamics*. Kessler E (1986) *Thunderstorms: A Social, Scientific, and Technological Documentary. Vol. 2: Thunderstorm Morphology and Dynamics*, 2nd edn., revised and enlarged. Norman, OK and London: University of Oklahoma Press. Adapted with permission from Lemon LR and Doswell III CA (1979) Severe thunderstorm evolution and mesocyclone structure as related to tornadogenesis. *Monthly Weather Reviews* 107: 1184–1197.)

multicells, or supercells. In the following, we review the basic physical processes that contribute to the wide spectrum of observed convective storm properties.

Buoyancy Effects

Convective storms differ dynamically from larger-scale atmospheric phenomena primarily due to the much stronger vertical accelerations and resulting vertical motions (both upward and downward) that are produced. Thus, the most fundamental equation relevant to convective storm dynamics is the non-hydrostatic vertical momentum equation:

$$\frac{dw}{dt} = -C_p\bar{\theta}_v\frac{\partial\pi}{\partial z} + B \qquad [1]$$

where π is a nondimensional form of the pressure, referred to as the Exner function,

$$\pi \equiv \left(\frac{p}{p_0}\right)^{R_d/C_p} \qquad [2]$$

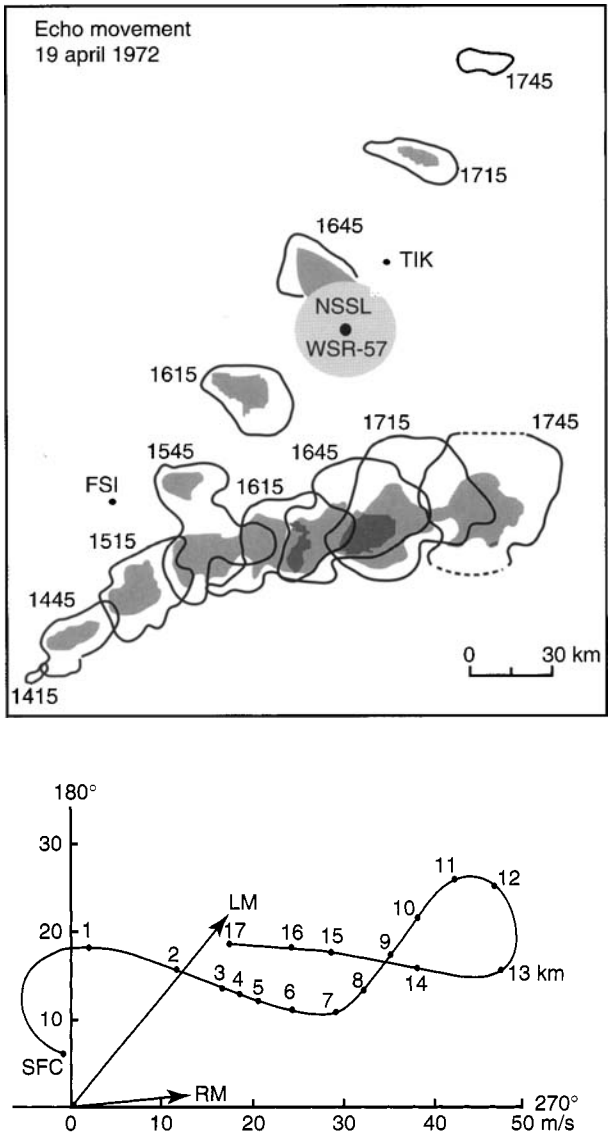

Figure 6 (Top) WSR-57 radar history of a splitting storm observed in south central Oklahoma. The solid contours indicate return greater than 10 dBZ, and the stippled regions indicate a return greater than 40 dBZ. Times adjacent to each outline are CST. (Bottom) A hodograph representative of the storm's environment. RM and LM indicate the observed motion of the right-moving and left-moving cells. (Adapted with permission from Burgess DW (1974) *Study of a Right-Moving Thunderstorm Utilizing New Single Doppler Radar Evidence.* Master's thesis, Department of Meteorology, University of Oklahoma.

and B is the buoyancy, including the effects of water vapor and precipitation loading:

$$B \equiv g\left[\frac{\theta'}{\bar{\theta}} + 0.61(q_v - \bar{q}_v) - q_c - q_r\right] \qquad [3]$$

In these equations, C_p represents the specific heat at constant pressure, p_0 is a reference surface pressure, R_d is gas constant for dry air, θ represents the potential temperature, q_v represents the water vapor mixing ratio, and q_c, q_r, and q_i represent cloud water, rainwater, and ice mixing ratios, respectively.

For an undisturbed environment (e.g., characterized by no variation of wind with height), the pressure contributions to vertical accelerations are usually very small relative to the buoyancy contributions, and are neglected. Under this assumption, an estimate of potential updraft (and downdraft) strength in a convective storm is often made by integrating the potential temperature contributions from buoyancy along a representative parcel path. For an updraft parcel, this quantity is referred to as the convective available potential energy (CAPE):

$$\text{CAPE} = \int_{\text{LFC}}^{\text{EL}} g\left(\frac{\theta'(z)}{\bar{\theta}(z)}\right) dz \qquad [4]$$

where $\theta'(z)$defines the potential temperature of a representative adiabatically ascending surface parcel, $\bar{\theta}(z)$ defines the environmental potential temperature profile, and the integral is taken over the vertical interval where the lifted parcel is warmer than its environment (usually from the level of free convection, LFC, to the equilibrium level, EL). This calculation is equivalent to evaluating the positive area represented on a skew-T diagram. Maximum potential temperature excesses in convective updrafts can be greater than 10 K, with magnitudes of CAPE larger than 6000 $m^2 s^{-2}$, but generally potential temperature excesses range between 3 and 6 K, with CAPEs of 1500 and 2500 $m^2 s^{-2}$ for moderately unstable convective days. A similar quantity can be calculated for downdraft parcels, and is referred to as DCAPE (downdraft CAPE).

By equating this CAPE (DCAPE) to vertical kinetic energy, one can then estimate the maximum updraft (downdraft) that would be expected from a given environment:

$$W_{\max} = (2 \times \text{CAPE})^{1/2} \qquad [5]$$

Using this relationship, a CAPE of 2500 $m^2 s^{-2}$ would translate to a maximum possible updraft strength of 70 $m s^{-1}$. However, water loading, perturbed vertical pressure gradients, and mixing effects reduce these estimates by roughly 50%. Vertical motions of 60 $m s^{-1}$ or greater have been observed in the strongest storm updrafts, but maximum downdrafts rarely exceed 30 $m s^{-1}$.

Vertical Wind Shear Effects

While the thermodynamic structure influences strongly the vertical accelerations in a convective

storm, vertical wind shear has a strong influence on what form convection might take. In particular, short-lived ordinary cells tend to be the preferred mode of organization in weak wind shear regimes, while multicells and supercells become the respective preferred mode of organization for increasing magnitude of vertical wind shear.

The characteristics of the wind profile in this regard are best represented in the from of a hodograph, where the wind vectors at each height are plotted from the origin, and then the tips of the vectors are connected to produce a hodograph trace (**Figure 7**). Vertical wind shear vectors are everywhere tangent to this hodograph trace, with the length of the hodograph curve over a given depth being a direct measure of the magnitude of the wind shear over that depth.

The relationship between wind shear and basic storm type is demonstrated in **Figure 8**, which depicts composite hodographs from a study of hailstorms in Alberta, showing an increasing length of the hodograph (especially over the lowest 6 km agl) as the type of convection progresses from short-lived storms to supercells. Generally, multicell storms become more prevalent when the length of the hodograph over the lowest 4–6 km agl is greater than 10–15 m s^{-1}, with supercells becoming more prevalent when the length of the hodograph is greater than 20–25 m s^{-1} over the lowest 4–6 km agl. Also included on the hodograph plots are observed cell motions. For ordinary cells and multiple-cell systems, cell motion tends to be with the mean wind over the lower 6–8 km of the profile, appearing on or near the hodograph trace. For the supercell, however, cell motion is well off the hodograph, well to the right of a calculated mean wind from the profile. Similar off-hodograph propagation is evident for the 19 April splitting storm (**Figure 6**), and reflects the unique dynamical character of supercell storms, as will be described below.

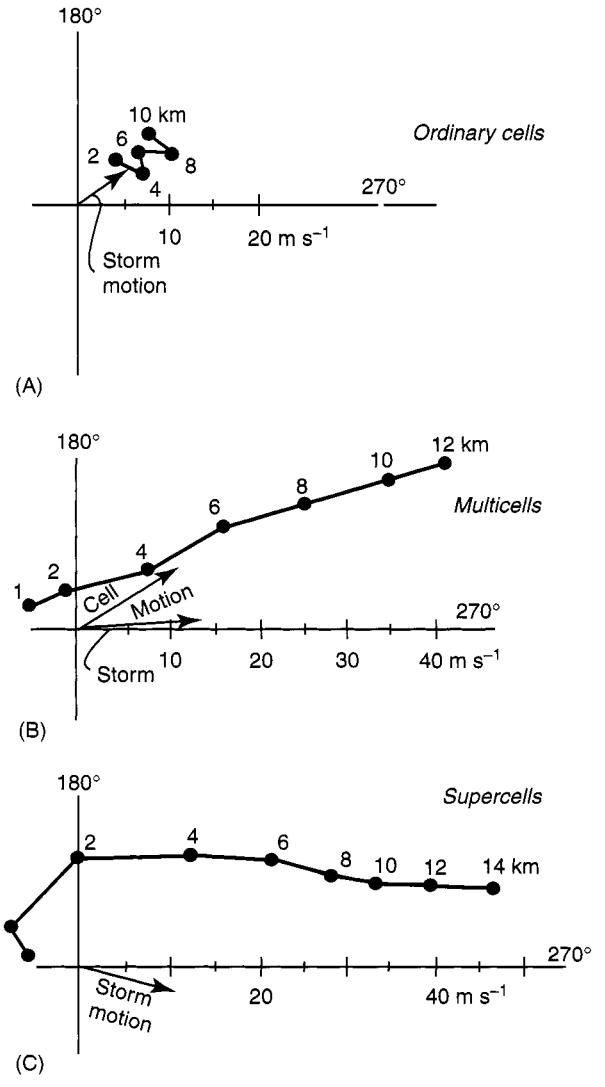

Figure 8 Typical wind hodographs for (A) ordinary cell, (B) multicell, and (C) supercell storms observed during the Alberta Hail Studies project. (Adapted with permission from Chisholm AJ and Renick JH (1972) *The Kinematics of multicell and supercell Alberta hailstorms.* Alberta Hail Studies, Research Council of Alberta Hail Studies, Rep. 72-2, Edmonton, Canada, pp. 24–31.)

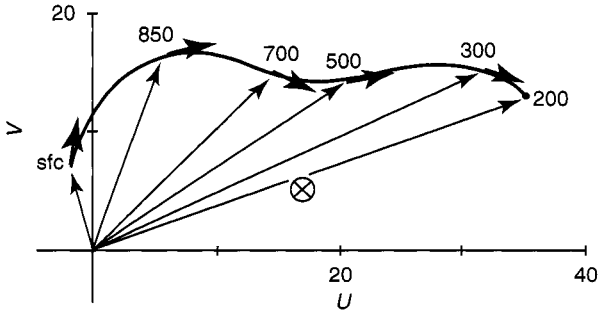

Figure 7 Composite hodograph (m s^{-1}) for tornadic supercell storms. Light arrows represent the wind vectors at each level, and heavy arrows indicate the direction of the shear vector at each level (labeled in mbar). The estimated mean storm motion is denoted by an encircled X. (Reproduced with permission from Klemp JB (1987) Dynamics of tornadic thunderstorms. *Annual Reviews of Fluid Mechanics* 19: 369–402. Adapted with permission from Maddox RA (1976) An evaluation of tornado proximity wind and stability data. *Monthly Weather Reviews* 104: 133–142.)

Two physical mechanisms help explain the organizational capacity of vertical wind shear. The first is related to the ability of a cold pool to trigger new convective cells. The second is related to the interaction of an updraft with the environmental vertical wind shear to produce an enhanced, quasi-steady storm structure.

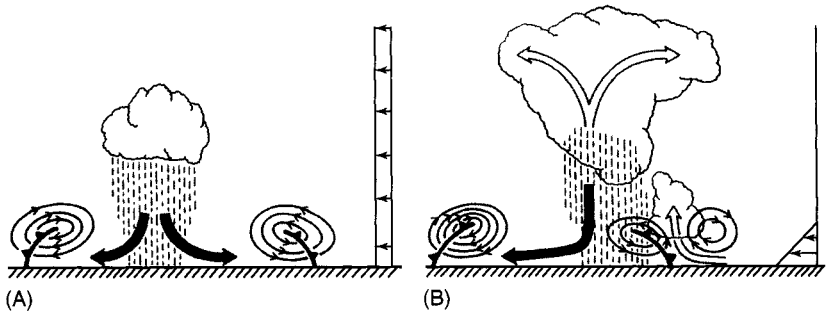

Figure 9 Schematics of cold pool–shear interactions. (A) A convective cell in a zero-shear environment produces a cold pool that propagates away from the cell. Without the presence of low-level shear, the circulation of the spreading cold pool inhibits deep lifting, and is less apt to trigger a new convective cell. (B) The presence of low-level shear counteracts the circulation of the cold pool on the downshear side, promoting deeper lifting and an enhanced potential to trigger new convective cells. (Adapted with permission from Rotunno R, Klemp JB, and Weisman ML (1988) A theory for strong, long-lived squall lines. *Journal of the Atmospheric Sciences* 45: 463–485.)

(i) *Cold Pool–Shear Interactions*: Cold pools are one of the most prominent features of convective storms, and have a critical role in determining whether a storm system can be maintained over a long period of time. This is due primarily to the ability of the cold pool to lift the surrounding air mass, thus serving potentially as a trigger for new convective cells. For a zero wind shear environment, the lifting along the leading edge of a cold pool is generally restricted to the depth of the cold pool's nose, as the circulation generated by the cold pool rapidly drags the lifted air rearwards. If the LFC is significantly higher than the nose of the cold pool, then it is unlikely that new cells can be triggered as the cold pool propagates away from a given cell (e.g., **Figure 9A**).

This picture changes significantly with the addition of environmental low-level vertical wind shear. Associated with this vertical wind shear is an opposing circulation that can balance the circulation of the cold pool somewhat on its downshear side, producing a more vertically oriented jet of air and deeper lifting at its leading edge (e.g., **Figure 9B**). An 'optimal' state for lifting along the cold pool can be envisioned when the circulation generated by the cold pool matches the opposite circulation associated with the environmental vertical wind shear. The depth/layer of vertical wind shear most important to this process is equivalent to the depth of the cold pool itself, but deeper shear layers will also contribute somewhat to this process. Ambient shear can further enhance the strength of new cells by virtue of the fact that such cells will move downshear along with the cold pool, increasing both the relative inflow into these cells and the time over which the cells maintain their low-level convergence and feed on the warm air ahead of the gust front. All in all, the strength and longevity of multiple-cell convective systems is enhanced for increasing magnitudes of ambient vertical wind shear, due primarily to the enhanced ability of the cold pool to trigger new cells.

(ii) *Updraft–Shear Interactions*: Vertical wind shear can further contribute to convective storm strength, organization, and sustenance through the interaction of the sheared flow with the convective updrafts. These effects can be both positive and negative. The negative effects are most clearly evident during the early stages of a storm's life, as clouds are observed to lean over in the direction of the mean tropospheric shear vector. This process takes vertical kinetic energy out of the accelerating buoyant plume, converting it to horizontal kinetic energy. If the shear is too strong relative to the buoyancy, a cloud can be literally torn apart.

The positive attributes of the shear are most clearly associated with the development of rotation about a vertical axis within the storm. This rotation originates through the tilting of horizontal vorticity inherent in the vertically sheared flow, as can be shown from the vertical vorticity equation:

$$\frac{d\zeta}{dt} = \omega_H \cdot \nabla_H w + \zeta \frac{\partial w}{\partial z} \qquad [6]$$

where ω_H and ζ represent the horizontal and vertical components of vorticity, respectively. This process is visualized in **Figure 10A**, for an isolated updraft developing in a unidirectionally sheared flow. The updraft initially deforms the ambient vortex lines upwards, leading to the development of a vortex couplet at midlevels, centered on the updraft. Cyclonic vorticity is generated on the right flank of the updraft (relative to the direction of the shear vector), with anticyclonic vertical vorticity on the left flank.

The main impact of this rotation on storm structure occurs through the relationship between the velocity

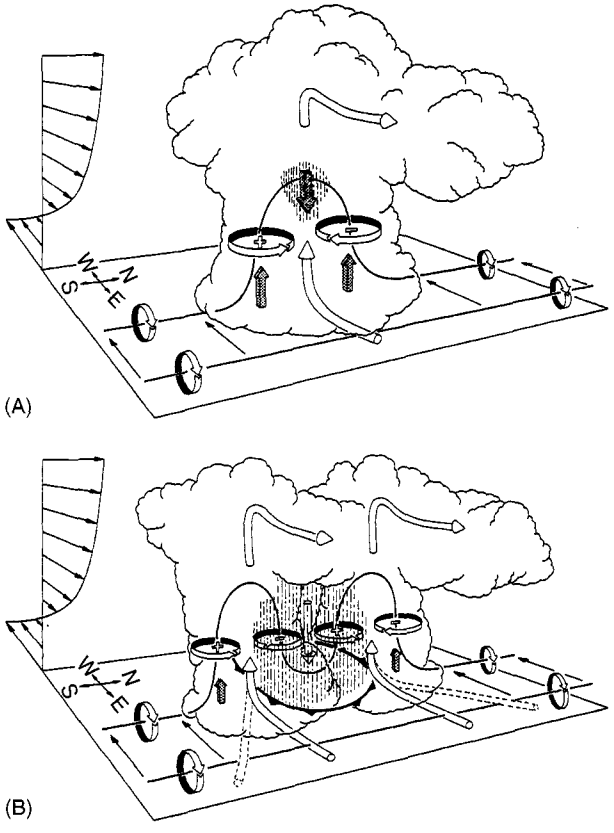

Figure 10 Schematic depicting how a typical vortex tube contained within (westerly) environmental shear is deformed as it interacts with a convective cell (viewed from the south-east). Cylindrical arrows show the direction of cloud-relative airflow, and heavy solid lines represent vortex lines with the sense of rotation indicated by circular arrows. Shaded arrows represent the forcing influences that promote new updraft and downdraft growth. Vertical dashed lines denote regions of precipitation. (A) Initial stage: vortex tube loops into the vertical as it is swept into the updraft. (B) Splitting stage: downdraft forming between the splitting updraft cells tilts vortex tubes downward, producing two vortex pairs. A new updraft is forced on the flanks of the splitting cell in response to upward-directed vertical pressure gradient forcing associated with the midlevel rotation. The barbed line at the surface marks the boundary of the cold air spreading out beneath the storm. (Reproduced with permission from Klemp JB (1987) Dynamics of tornadic thunderstorms. *Annual Reviews of Fluid Mechanics* 19: 369–402.)

field and the pressure field. In particular, the localized development of rotation in a fluid is associated with lowered pressures (e.g., consider what happens when you stir a cup of coffee). For convective scales of motion, this lowering of pressure occurs whether the rotation is cyclonic or anticyclonic. If the resulting rotation at midlevels in a storm is sufficiently strong (e.g., if the storm is developing in a sufficiently sheared environment), the induced pressure deficits at midlevels will produce a significant upward-directed vertical pressure gradient force that will force the updraft to propagate to both flanks of the original cell.

Once the updrafts propagate to the flanks (**Figure 10B**), they become more colocated with the midlevel rotation centers, which are then further enhanced by vortex stretching. The vortex tilting process continues to generate new rotation on the flanks of the storm, and the updrafts will continue to propagate towards these midlevel rotational centers. Thus, the original cell splits into mirror image cyclonic and anticyclonic storms that propagate to the right and left of the shear vector, respectively. This is the most basic process by which supercell storms may be generated and sustained.

The relationship between the velocity and pressure fields in a convective storm can be derived by taking the divergence of the momentum equations, assuming incompressibility, which leads to the following Poisson equation for the nondimensional pressure, π:

$$\nabla \cdot \left(C_p \bar{\rho} \bar{\theta}_v \nabla \pi\right) = -\nabla \cdot (\bar{\rho}\mathbf{v} \cdot \nabla \mathbf{v}) + \frac{\partial B}{\partial z} \qquad [7]$$

This equation can be solved for the contributions to the perturbation pressure field from the velocity and buoyancy terms on the right-hand side of eqn [7] individually, allowing the vertical momentum equation [1] to be rewritten to reflect the contributions from velocity-related pressure perturbations and buoyancy-related processes individually as well:

$$\frac{dw}{dt} = -C_p \bar{\theta}_v \frac{\partial \pi_{dn}}{\partial z} + \left(-C_p \bar{\theta}_v \frac{\partial \pi_b}{\partial z} + B\right) \qquad [8]$$

The first term on the right-hand side of eqn [8] is referred to as the dynamic contribution to vertical acceleration, and includes all the effects of shear on an updraft, such as the initial tendencies for a cell to lean in the direction of the shear as well as the positive influences due to the development of rotation. The second term on the right-hand side of eqn [8] includes the usual effects of buoyancy as well as the compensating effects due to the buoyant contributions to the pressure field. For ordinary convective cells, which develop in weakly sheared environments, the buoyancy terms generally contribute 60–70% of the maximum updraft strength in a storm. However, the supercell storms, which develop in strongly sheared environments, 60–70% of the maximum updraft strength can come from the dynamic contributions, with most of this contribution coming in the lowest several kilometers of the storm. This explains why supercell storms can be unusually strong, and can persist, sometimes even in the presence of significant

low-level capping inversions, as are generally observed at night.

The updraft–shear interaction processes described above are symmetric about the ambient shear vector for unidirectionally sheared environments (e.g., shear environments characterized by a straight line on a hodograph). In such cases, mirror image supercells propagating off the hodograph to the right and left of the shear vector can be produced, as demonstrated in idealized cloud model simulations presented in **Figure 11A**. This symmetry is modified, however, by the addition of directional shear to the environment. If the environmental vertical wind shear vector turns clockwise with height over the lowest few kilometers agl (referred to as a clockwise curved hodograph), as presented in **Figure 11B**, the pressure forcing is enhanced on the cyclonic flank of the original cell, and a dominant cyclonically rotating supercell results from the original splitting process. However, if the environmental vertical wind shear turns counterclockwise with height (not shown), the anticyclonic member of the original split would have been favored instead. Climatologically, environmental hodographs in the vicinity of supercell storms exhibit cyclonic turning of the shear vector at low levels (e.g., consider the hodographs in **Figures 7** and **8C**), and thus cyclonically rotating supercells tend to be more common and dominant than anticyclonically rotating supercells.

Figure 12 presents the overall flow structure for a mature, cyclonically rotating supercell storm. An anticyclonically rotating supercell is the mirror image of this. The flow vectors depict the main interwoven airstreams, with the low-level flow converging from both ahead and behind of the surface gust front and rising into a deep, rotating updraft, and the midlevel flow passing in front of and then descending behind the updraft. The updraft reaches the top of the storm, where it then diverges within the anvil, primarily in the downshear direction. While the midlevel rotation in the storm is generated via the tilting of horizontal vorticity associated with the warm, ambient environment (e.g., **Figure 10A**), the air that feeds the low-level rotation originates largely from the cold side of the surface cold pool boundary. Horizontal vorticity is generated in response to the buoyancy gradients across this boundary, as depicted by the low-level vortex lines turning towards the storm on the cold side of the forward flank gust front, and this horizontal vorticity feeds into the low-level updraft in a streamwise sense, leading to the low-level updraft rotation. It is this low-level, rotating updraft that leads to the development of significant tornadoes within supercell storms.

Summary

For convective storms, cold pool generated lifting and dynamic pressure forcing work together to produce the observed storm characteristics. The relative importance of each mechanism is dependent on the characteristics of the thermodynamic profile as well as the vertical wind shear profile of the environment in which the storm grows. A convective system may be composed of both ordinary cells and supercells simultaneously, while maintaining a general multicell character. Storm types also have a tendency to change during the lifetime of an event. For instance, an isolated supercell will often evolve into a more multicellular line of ordinary cells over time as the storm generated cold pool and associated lifting becomes stronger and begins to dominate over the dynamic lifting effects associated with the rotating updraft. In such cases, a supercell is said to have 'gusted out' or 'lined out'. Convective storms also change character as they move into a different mesoscale environment, or when they interact with each other, as within a squall line.

While convective updraft characteristics can generally be anticipated quite well from environmental thermodynamic and shear profiles, potential downdraft and resulting cold pool characteristics are much more difficult to gauge from environmental conditions. The storm-generated downdraft and cold pool is certainly sensitive to the amount of thermodynamic instability and the distribution of moisture in the environment, but it is also sensitive to the characteristics of the precipitation that is produced within the storm. For instance, a convective cloud that predominantly produces a few large raindrops or hailstones will tend to have a weaker downdraft and cold pool than a cloud that produces a large quantity of smaller drops, due to decreased evaporation rates. Along these lines, supercell storms have been subclassified into high-precipitation (HP), classic, and low-precipitation (LP) varieties, based on intensity and distribution of the precipitation and the resulting strength of the system-generated cold pool. Many of these factors are discussed in companion chapters within this volume.

Climatology of Convective Storm Types

Ordinary cell and multicell storm systems are commonly observed from the tropics through midlatitudes, whenever thermodynamic instability exists and there is a sufficient triggering mechanism for the convection. Supercell storms, however, tend to be more limited to midlatitude, continental regions,

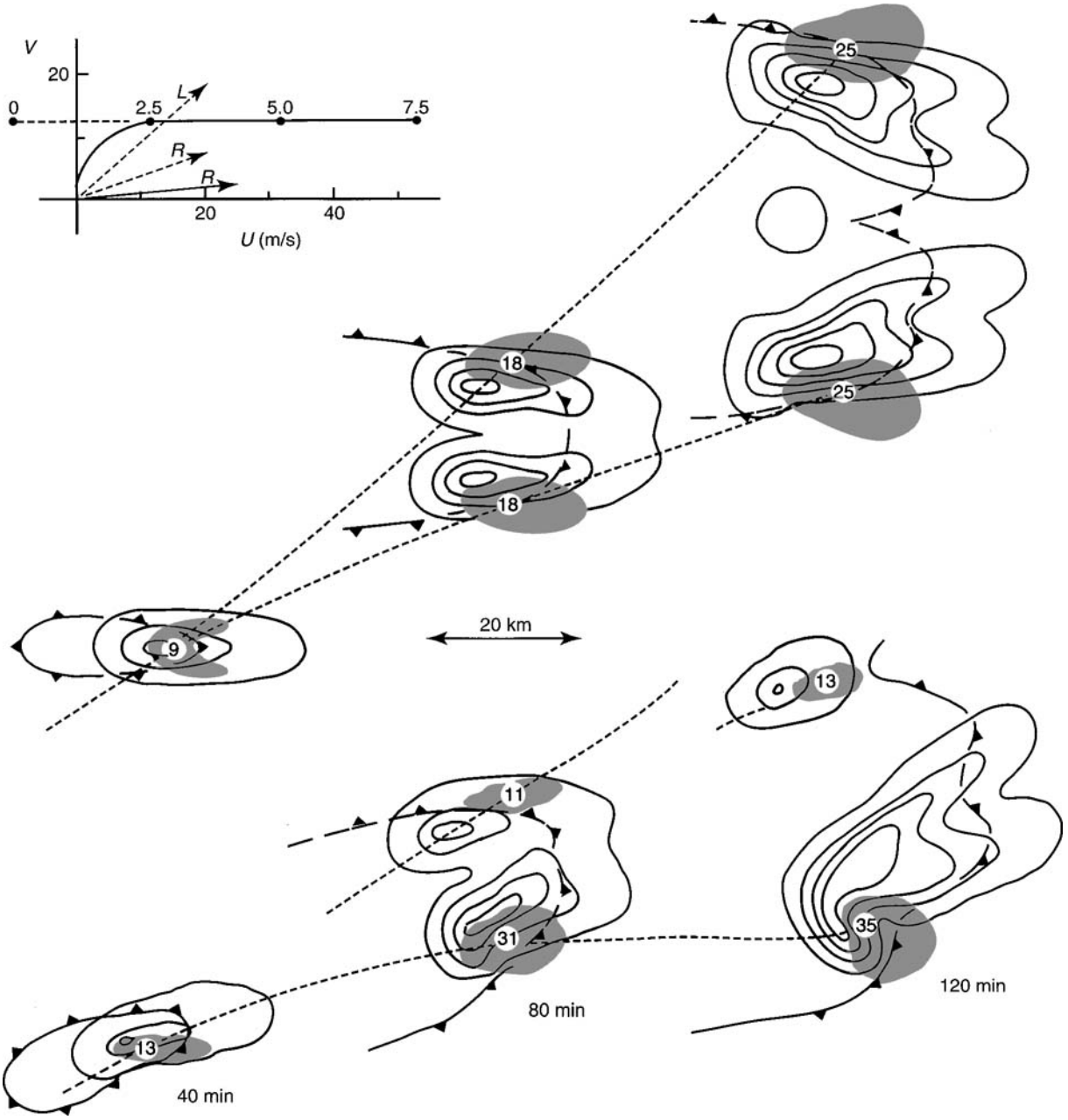

Figure 11 Plan views of numerically simulated convective storms at 40, 80, and 120 min for two environmental wind profiles (displayed at the upper left) having wind shear between the surface and 7.5 km agl. The storm system in the lower portion of the figure evolves in response to the wind profile for which the vertical wind shear vector turns clockwise with height between the ground and 2.5 km (heavy solid line in the hodograph), while the upper system develops when the shear is unidirectional (same wind profile except follow the heavy dashed line below 2.5 km). The plan view depicts the low-level (1.8 km) rainwater field (similar to radar reflectivity) contoured at 2 g kg^{-1} intervals, the midlevel (4.6 km) updraft (shaded regions), and the location of the surface cold pool boundary (barbed lines). The maximum updraft velocity is labeled (in m s^{-1}) within each updraft at each time. The dashed lines track the path of each updraft center. Arrows on the hodograph indicate the supercell propagation velocities for the unidirectional (dashed) and turning (solid) wind shear profiles. (Reproduced with permission from Klemp JB (1987) Dynamics of tornadic thunderstorms. *Annual Reviews of Fluid Mechanics* 19: 369–402.)

where sufficient vertical wind shear can exist in association with thermodynamic instability. Supercell storms are especially prevalent in the spring and early summer in the plains and mid-western regions of the United States, where the Gulf of Mexico supplies a source of low-level moisture to enhance thermodynamic instability, and the frequent passage of synoptic-scale waves offers a source for the vertical wind shear. The frequency of supercell storms and the associated tornadoes in this part of the United States

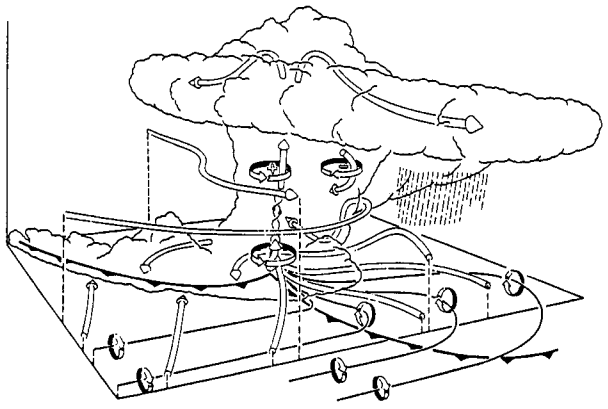

Figure 12 Three-dimensional schematic view of a mature supercell thunderstorm at a stage when low-level rotation is intensifying. The storm, viewed from the south-east, is evolving in westerly environmental wind shear. The cylindrical arrows depict the flow in and around the storm. The thick lines show the low-level vortex lines, with the sense of rotation indicated by the circular-ribbon arrows. The heavy barbed line marks the boundary of the cold air beneath the storm. (Reproduced with permission from Klemp JB (1987) Dynamics of tornadic thunderstorms. *Annual Reviews of Fluid Mechanics* 19: 369–402.)

has led to this region being referred to as 'Tornado Alley.'

Supercell storms can also be embedded within the rain bands of landfalling tropical storms and hurricanes. These supercells tend to be shallower than more classic supercells, as minimal instability (CAPE less than $1000\,J\,kg^{-1}$) is available within the associated tropical air mass. However, very strong low-level vertical wind shears are generated as the rain bands come ashore, and very intense (of order $10\,m\,s^{-1}$) updrafts can be generated in the lowest 1–2 km agl in such cells, due to the dynamic vertical pressure gradients associated with the rotating updrafts. Such shallow supercells are hypothesized to be the source of tornado outbreaks within landfalling tropical storms and hurricanes.

In the midlatitudes, convection often occurs in the warm sectors of synoptic-scale waves, in association with cold fronts and warm fronts. In the tropics, convective activity is commonly located along the intertropical convergence zone (ITCZ). In both the tropics and midlatitudes, convection also commonly occurs along sea breeze fronts or in association with topographic features such as mountain ridges. Generally, oceanic convection tends to be weaker than continental convection, due to less thermodynamic instability over oceanic regions. Convective storms can occur at any time of the day or night, when thermodynamic instability and a trigger is available, but severe convection tends to maximize in the late afternoon and evening hours, in response to the enhanced thermodynamic instability associated with diurnal heating.

See also

Bow Echos and Derecho. **Convective Storms:** Convective Initiation. **Density Currents**. **Gust Fronts**. **Hail and Hailstorms**. **Mesoscale Meteorology:** Cloud and Precipitation Bands. **Tornados**. **Waterspouts**. **Weather Prediction:** Severe Weather Forecasting.

Further Reading

Browning KA (1977) The structure and mechanism of hailstorms. *Hail: A Review of Hail Science and Hail Suppression, Meteorological, Monographs*, vol. 16, pp. 1–43. Boston: American Meteorological Society.

Byers HR and Braham RR Jr (1949) *The Thunderstorm*. Supt of Documents, Washington, DC: US Government Printing Office.

Church C, Burgess D, Doswell C and Davies-Jones R (1993) The tornado: its structure, dynamics, prediction, and hazards. *Geophysical Monographs* 79: 637.

Doswell III CA (1985) *The Operational Meteorology of Convective Weather. Volume II: Storm Scale Analysis*. NOAA Technical Memorandum ERL ESG-15.

Kessler E (1986) *Thunderstorms: A Social, Scientific, and Technological Documentary. Vol. 2: Thunderstorm Morphology and Dynamics*, 2nd edn., revised and enlarged. Norman, OK and London: University of Oklahoma Press.

Klemp JB (1987) Dynamics of tornadic thunderstorms. *Annual Reviews of Fluid Mechanics* 19: 369–402.

Lemon LR (1980) *Severe Thunderstorm Radar Identification Techniques and Warning Criteria*. NOAA Technical Memorandum, NWS NSSFC-3, Kansas City, MO (NTIS PB81-234809).

Rotunno R, Klemp JB and Weisman ML (1988) A theory for strong, long-lived squall lines. *Journal of the Atmospheric Sciences* 45: 463–485.

Weisman ML and Klemp JB (1986) Characteristics of isolated convective storms. *Mesoscale Meteorology and Forecasting*, pp. 331–358. Boston: American Meteorological Society.